Excited State Energy Relaxation in the FMO Complexes of the Green Bacterium *Prosthecochloris aestuarii* at Low Temperatures

Simone I. E. Vulto,* Alexander M. Streltsov,† and Thijs J. Aartsma

Biophysics Department, Huygens Laboratory, University of Leiden, P.O. Box 9504, 2300 RA Leiden, The Netherlands

Received: December 10, 1996; In Final Form: March 5, 1997[⊗]

Energy transfer processes at 10 K in the water-soluble bacteriochlorophyll *a*−protein complex (FMO complex) from the green bacterium *Prosthecochloris aestuarii* have been studied by femtosecond one- and two-color pump−probe measurements. Decay-associated spectra have been obtained for different excitation wavelengths. From these we conclude that energy relaxation occurs via a stepwise, cascading process down the Q_y manifold of energy states in the FMO complex. Observed time constants for these steps are 500 fs and 1.7, 5.5, and 30 ps and are correlated with the position in the Q_y manifold, becoming shorter with increasing energy. Anisotropy decay functions at different wavelengths exhibit two major components: one of ∼100 fs and one of ∼1 ps.

Introduction

Energy transfer in light-harvesting systems is a complex problem and has been studied extensively. Yet, it continues to be an increasingly active field of research as new and improved experimental methods can be applied and as more and more structural information becomes available.[1−4] In particular, the water-soluble bacteriochlorophyll *a* (BChl *a*) complex, which can be isolated from green sulfur bacteria, has always been of great interest because it was the first photosynthetic pigment−protein complex of which the structure was solved by X-ray crystallography.[1,5−8] As such, it has been a test case for theories of dipolar interactions and exciton calculations, [9−12] in particular the relation of such calculations—based on detailed structural information—to spectroscopic properties and to the excited state dynamics.

The BChl *a* complex, usually referred to as the FMO complex (after Fenna, Matthews, and Olson[5]), consists of three identical protein subunits in a configuration with C_3 symmetry. Each subunit contains 7 BChl *a* molecules to give a total of 21 for the FMO complex; no other pigments are present in the complex. The nearest-neighbor distances (center-to-center) within one subunit vary from 11.3 to 14.4 Å, while the distance is about 24 Å between nearest neighbors in different subunits of the trimer.

From the orientation of the BChl *a* molecules and of their transition moments, together with the distances between them, the pairwise dipolar interactions in the FMO complex can be calculated to give a maximum value of about 200 cm^{-1}.[10,11] By use of this information, the optical spectra have been calculated with the zero-order energies of the pigments as adjustable parameters. Reasonable simulations have been obtained for absorption and CD spectra,[9−11] but the same set of parameters does not give very good results for LD, T − S, and LD(T − S) spectra.[12,13] Nevertheless, it is clear that the spectrum of the Q_y absorption is not only determined by variations in site energies but also by large exciton shifts due to the dipolar interactions. This is also evident from the CD spectrum[14,15] and from the T − S spectrum,[13,16] which is more or less representative of the spectral changes when one of the 21 pigments would have been removed.

Energy relaxation at room temperature was studied with subpicosecond resolution by Savikhin and Struve[17,18] using time-resolved absorption spectroscopy and also by measuring the time-resolved anisotropy. The isotropic decays are characterized by time constants ranging from 100 to 900 fs, depending on wavelength, while the anisotropy decays with time constants of 75−135 fs and 1.4−2.0 ps. The origin of the fast anisotropy decay is uncertain, but nevertheless these data suggest rapid relaxation to lower energy states in the complex. The slower time constants have been attributed to equilibration among equivalent lowest energy pigments on different subunits in the trimer.

Hole-burning experiments in the Q_y band of FMO at 4 K were performed by Johnson and Small, [19,20] who reported time constants for dephasing of >20 ps (limited by spectral resolution) in the 825 nm band and of about 100 fs for wavelengths shorter than 820 nm. They suggested that the very fast dephasing was due to ultrafast exciton scattering within the manifold of exciton states within the Q_y band. The hole-burning data showed that the electron−phonon coupling is very weak in the FMO complex.

Another study at low temperature involved accumulated photon echo measurements,[21−23] which showed relatively long time constants for the coherent lifetimes of the optically excited states, in particular in the long-wavelength region of the Q_y absorption band of FMO. These coherent lifetimes were strongly dependent on the wavelength of excitation, decreasing from hundreds of picoseconds around 825 nm to less than 300 fs at 795 nm. A strong temperature dependence of the photon echo decay was also observed.

The results of these low-temperature measurements were interpreted in terms of the exciton structure of the FMO absorption band. There is agreement about the conclusion that excited state relaxation occurs to the lowest state in the manifold via downward exciton scattering. However, hole-burning[19,20] and accumulated photon echo measurements[21−23] arrive at different conclusions concerning the transition rates involved.

* To whom correspondence should be addressed. E-mail: vulto@biophys.leidenuniv.nl. Fax: 31-71-5275819.

† Permanent address: Laboratory of Photobiophysics, Belozersky Institute of Chemical and Physical Biology, Moscow State University, Moscow, 119899, Russian Federation.

⊗ Abstract published in *Advance ACS Abstracts,* May 1, 1997.

S1089-5647(96)04040-0 CCC: $14.00

To resolve this issue, we have performed time-resolved absorption difference spectroscopy at 10 K to obtain additional information about energy relaxation processes at low temperatures, with a time resolution of 80 fs. The results unambiguously show that excited state relaxation in the FMO complex is indeed a stepwise relaxation process down the ladder of exciton states. At least four major transitions can be distinguished, each with a different time constant, which correlate with the structure in the absorption spectrum.

Materials and Methods

The FMO complexes of *P. aestuarii* are isolated and purified as described by Francke.[24] Since the measurements were performed at 10 K or less, the sample was mixed with glycerol (70%) to obtain a clear glass upon cooling. The optical density was adjusted at room temperature to 0.7 at 809 nm in the 1 mm cuvette used in the experiment.

A mode-locked cavity-dumped Ti:sapphire laser was homebuilt according to the designs of Asaki et al.[25] and Pschenichnikov et al.[26] The laser was pumped by 5.5 W of an argon ion laser (Coherent Innova). The output of the laser was centered at a wavelength of 809 nm, with a bandwidth of 40 nm (fwhm) and a pulse duration of about 20 fs. The experimental setup was a pump−probe configuration with the excitation and probe beam adjusted at parallel, perpendicular, or magic angle polarization directions. This was achieved by rotation of a dispersion-compensated waveplate (CVI), which was installed in the excitation beam. Wavelengths of excitation were selected by inserting a narrow bandpass filter in the pump beam (6−8 nm fwhm, from CVI or Ferroperm). The probe beam was obtained by splitting off a fraction from the laser output beam. Both excitation and probe beams were precompensated for dispersion by double passing of two fused-silica prisms in the optical path. This resulted in an instrument response function of 80−100 fs, depending on the bandpass filter installed in the pump beam. The energy per excitation pulse was adjusted to about 0.2 nJ per pulse (10 μW, 0.03 mJ/cm^2) in order to avoid annihilation effects; at most 1−2% of the BChl *a* in the sample was excited. The absorbance changes were measured using the full 40 nm bandwidth of the probe beam, which was dispersed by a monochromator after passing through the sample, facilitating wavelength selective detection of absorbance changes. The repetition rate of the laser was reduced to 50 kHz by means of the cavity dumper to avoid triplet state accumulation, and the pump beam was additionally modulated at 500 Hz by a mechanical chopper. The probe beam was monitored after passing the monochromator by an integrating photodiode in combination with phase-sensitive detection referenced to the 500 Hz signal of the chopper. The sample was contained in an Oxford CF1204 flow cryostat and cooled to 10 K.

Results

The absorption spectrum of the FMO complex of *P. aestuarii* at 10 K is shown in Figure 1. The Q_y region contains at least five main bands at 793, 802, 806, 815, and 825 nm. We have performed time-resolved measurements of absorbance changes across the whole spectrum with a selection of four different wavelengths of excitation to match the most prominent bands in the absorption spectrum, although at the expense of time resolution. The spectral distribution of each of the four wavelength settings we have used is indicated in Figure 1. For reference, the positions of the exciton levels calculated by Gülen[12] to simulate the optical spectra of FMO are also indicated in Figure 1. From this picture it is quite clear that several exciton levels are excited simultaneously within the bandwidth

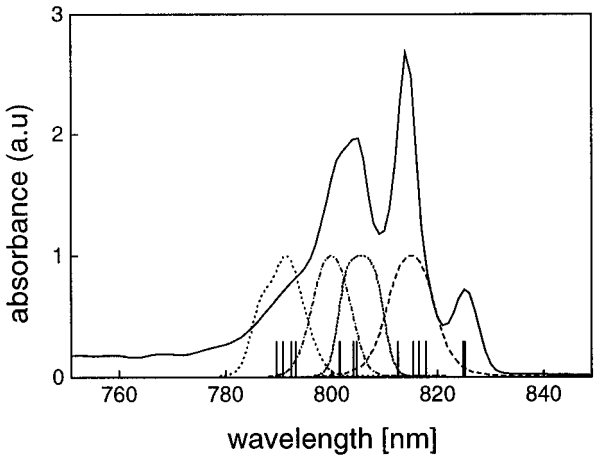

Figure 1. Absorption spectrum of the FMO protein of *P. aestuarii* at 10 K (solid). Also shown are the spectra of the excitation pulses centered at 790 (dotted), 800 (dot−dash), 806 (dashed), and 815 nm (long dashed). The sticks refer to the position of the exciton levels as calculated by Gülen[12] (see text).

of excitation at each of the four selected wavelengths. It was not useful to reduce the excitation bandwidth any further because this would limit the time resolution of the experiments too much, considering that some of the energy transfer steps occur on a sub-picosecond time scale.

The time dependence of absorbance changes was measured at different combinations of excitation and probe wavelengths to obtain information about the excited state dynamics of the FMO complex, related to energy transfer, in conjunction with the excitonic structure of the Q_y band. As an example, we show some of the isotropic kinetic traces we obtained with excitation at 806 nm in Figure 2. The wavelengths of detection (from parts A to E) were 790, 800, 806, 815, and 825 nm, respectively. The absorbance kinetics show a large variation of characteristic features as a function of wavelength of detection. To the blue of the excitation wavelength of 806 nm there is a significant contribution of induced absorption that is particularly evident in Figure 2A. At 800 nm (Figure 2B), we observe cancellation of bleaching and induced absorption of the component with the longer time constant so that only the faster one remains. Toward longer wavelengths the observed signal consists of a bleaching, although components of induced absorption are also present in this range as we will discuss further on. All the kinetic traces are multiexponential with varying combinations of decay and rise time components.

Figure 3 shows the time-resolved absorbance difference spectra of FMO complexes of *P. aestuarii* for excitation at 806 nm. Immediately after excitation the maximum is located at 806 nm, while an induced absorption is observed from 780 to 800 nm. At longer decays the maximum shifts to the red, with a corresponding shift of the induced absorption at the blue side of the spectrum. If we look in more detail, it is clear that at 1.7 ps delay the absorption around 806 nm has decreased while a bleaching develops at 815 and 825 nm. At 5.5 ps delay the bleaching around 825 has increased further, while at the same time the bleaching at 815 nm has started to decrease. At 25 ps delay, the absorbance difference spectrum is dominated by a bleaching at 825 nm, and the induced absorption on the blue side of the spectrum is nearly zero. The time development of the absorbance difference spectrum indicates an energy transfer toward energy states in the Q_y manifold absorbing at longer wavelengths. After a delay of 37 ps no significant spectral changes in transient absorption are observed, except for a decay of the bleaching at 825 nm, because of relaxation to the ground

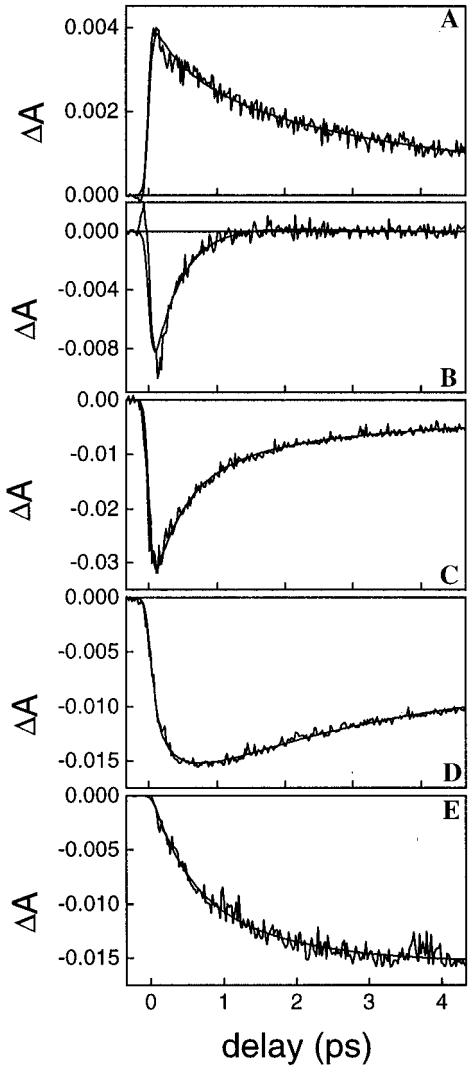

Figure 2. Time-resolved isotropic absorbance difference profiles for excitation at 806 nm and detection at (A) 790, (B) 800, (C) 806, (D) 815 nm, and (E) 825 nm.

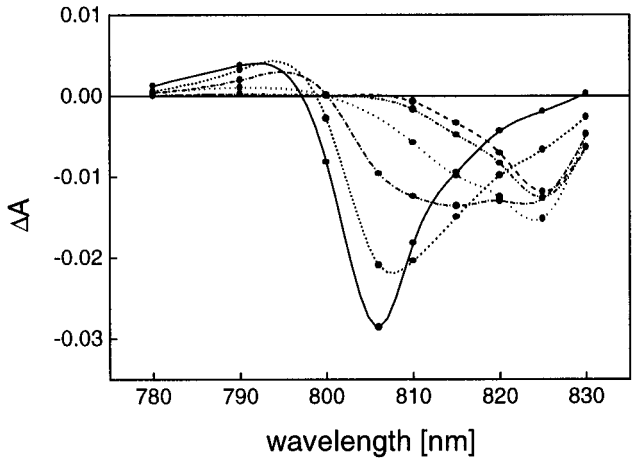

Figure 3. Absorbance difference spectra at specific time delays for excitation at 806 nm. The following delays of the probe pulse are plotted: 0.1 (solid), 0.5 (dashed), 1.7 (dot−dash), 5.5 (dotted), 25 (dot−dot−dash) and 37 (long-dashed) ps.

state. We therefore conclude that the absorbance difference spectrum is fully equilibrated in about 40 ps.

Similar kinetics are observed at other excitation wavelengths, although the specific details, of course, vary for each of these data sets. From multiexponential fits of these kinetic traces it

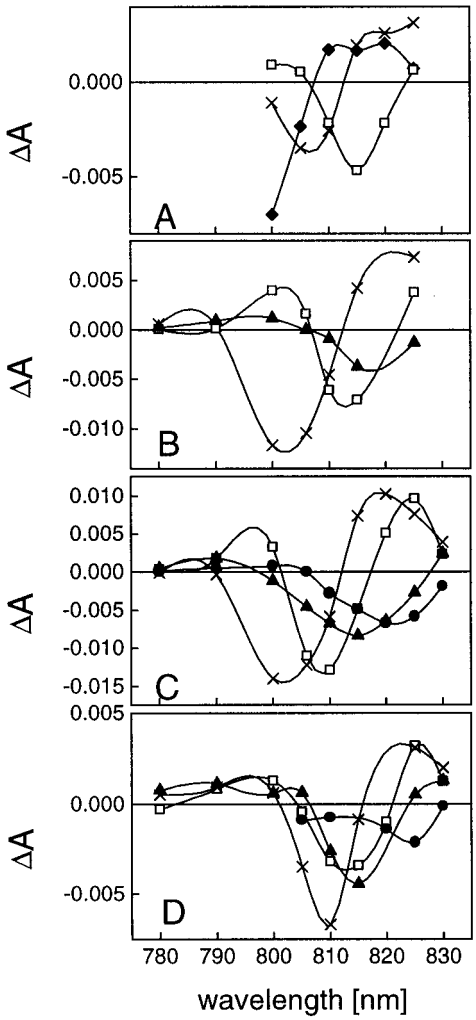

Figure 4. Decay-associated spectra of FMO complexes of *P. aestuarii* at the following excitation wavelengths: (A) 790, (B) 800, (C) 806, and (D) 815 nm. Time constants associated with the spectra are <100 fs (◆), 0.5 ps (×), 1.7 ps (□), 5.5 ps (▲), and 37 ps (●).

was apparent that they can all be characterized by a limited set of time constants. In Figure 2 we only show the absorbance kinetics over a time range of 5 ps, but in all cases we also obtained a similar data set over a time range of 50 ps in order to determine more accurately the longer time constants.

To obtain a meaningful and consistent analysis of this extensive data set, we applied a global fitting program that was based on the algorithm described by Beechem et al.[27] From this analysis we found that all kinetic traces can be fitted very well by a linear combination of exponentially decaying functions, of which the most important components have time constants of 0.5, 1.7, 5.5, and 37 ps. To correct for coherent artifacts around $t = 0$ in some of the data, a short component was included as well. Measurements over a longer time span (500 ps, data not shown) showed that a longer component is also present with a time constant on the order of 1 ns. It is known from fluorescence measurements that the excited state of FMO decays to the ground state with a time constant of 2 ns at 77 K.[28] At the time scale of the experiments we present here, of 5 and 50 ps, the contributions of this nanosecond component were considered to be constant.

The amplitudes of the different decay components, resulting directly from the global fitting procedure, were plotted as a function of probe wavelengths to obtain the corresponding decay-associated spectra (DAS). Figure 4 shows the DAS of each of the relevant components in the decay of FMO with

excitation at 790, 800, 806, and 815 nm, respectively. These DAS spectra should be interpreted as follows. A negative value in the DAS represents the amplitude of the decay of a bleaching or that of the appearance of an induced absorption. A positive value is associated with the rise of a bleaching or the decay of an induced absorption.

The DAS spectra for excitation at 790 nm (Figure 4A) are dominated by a decay of less than 100 fs for the initial bleaching at 790 nm, while the same time constant is observed in the appearance of a bleaching at longer wavelengths. The subsequent decay of the bleaching at 805 nm in 500 fs is correlated with the appearance of a bleaching that extends from 815 to 825 nm. The bleached band at 815 nm then decays in 1.7 ps. Note that the latter decay is accompanied by that of an induced absorption around 800 nm.

The 500 fs time constant is also very prominent in the decay of the initial bleaching at 800 nm, with excitation also occuring at this wavelength (Figure 4B), and in the rise time of the bleaching at wavelengths longer than 815 nm. Here, we also observe the appearance of a bleaching at 815 nm followed by a decay in 5.5 ps. The 1.7 ps component is also present in the decay and appearance of bleachings at 810, 815, and 825 nm and in the decay of an induced absorption around 800 nm.

All four time constants are observed very distinctly in the DAS with excitation at 806 nm (Figure 4C). The bleachings with the three shortest time constants have a maximum at more or less the same wavelengths as in parts A and B of Figure >4, while the 37 ps component is observed as a bleaching centered at 825 nm. From inspection of the initial amplitudes, it is clear that the bleachings at 800 and at 810 nm are generated by direct excitation. The general features and time-development of the energy transfer processes are consistent with the absorbance difference profiles as shown in Figure 3.

The bandwidth of excitation at 815 nm is relatively broad (see Figure 1) so that multiple bands are excited directly. This is reflected in the initial bleaching, the decay of which contains three lifetime components with corresponding rise times for bleaching between 820 and 830 nm. The bleaching of the 0.5 ps components is significantly red-shifted compared to bleachings in parts A−C of Figure 4. Note that the 37 ps component is also present as the rise time of an induced absorption around 810 nm.

In Figure 5 we show the kinetics of absorbance changes obtained with parallel and perpendicular polarization of excitation and probe pulses in one-color pump−probe measurements at 806 nm (Figure 5A) and at 815 nm (Figure 5B). From these measurements we have determined the anisotropy at these two wavelengths, shown in parts C and D of Figure 5. At 806 nm the anisotropy starts at 0.4 and decays biexponentially to a value of 0.15 with time constants of 100 and 700 fs. A longer component of 3−5 ps may also be present, but this one is difficult to determine given the signal-to-noise ratio and the limited fitting window. At 815 nm the anisotropy also decays biexponentially from a value of 0.4 to a value of 0.20 with time constants of 70 and 900 fs. In this case, inclusion of additional components does not significantly improve the quality of the fit.

Discussion

The various time constants that describe the time dependence of the absorbance changes created by optical excitation of the FMO complex are observed as decay times as well as rise times, in bleaching and in induced absorption. This indicates that the characteristic features of this time dependence are determined by correlated processes. The observation of decay and rise time components with identical time constants at different probe wavelengths is characteristic of an energy transfer process.

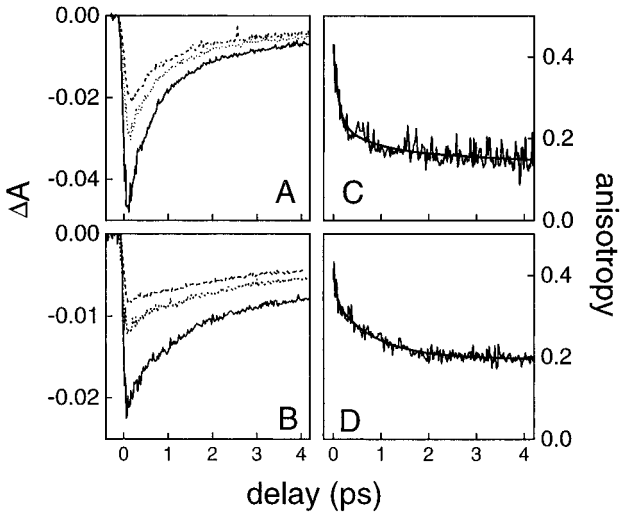

Figure 5. One-color absorption difference profiles at (A) 806 and (B) 815 nm for parallel (solid), perpendicular (dashed), and magic angle (dotted) polarizations, and anisotropy decay functions $r(t)$ at (C) 806 and (D) 815 nm.

Apart from a very short-lived component (<100 fs) at the very blue edge of the Q_y absorption band and a very long-lived component at the very red edge (>800 ps), we have identified four time constants that dominate the excited state dynamics of FMO upon excitation in the region of 790−815 nm: 0.5, 1.7, 5.5, and 37 ps. The time constant of ∼100 fs may well be attributed to excitation of a vibronic band that may constitute the main contribution to the absorption spectrum around 790 nm. The long-lived component of >800 ps represents the time constant for decay to the ground state. Considering that the four other time constants are observed as decay times as well as rise times of bleachings, we conclude that they are associated with energy transfer processes. The data also show that these time constants each have a maximum amplitude at a particular wavelength in the decay-associated spectra, certainly if we look at the wavelength distribution of initial bleaching but also to some degree in that of the rise times. This implies that the time constants can be attributed to energy transfer processes, or energy relaxation, between specific energy states (or groups of energy states) within the Q_y manifold.

The time constants of 0.5, 1.7, 5.5, and 37 ps determined from the extensive data sets in our experiments are of the same order of magnitude as recently described by Savikhin and Struve[29] with pump−probe measurements on FMO complexes of *Chlorobium tepidum* at 19 K. From measurements at two pump and probe wavelengths, Savikhin and Struve[29] obtained four time constants of ∼600 fs and 3−5, 13−50, and 200−1000 ps with spectral equilibration in 19 ps, where we observe at least 37 ps for a full equilibration (Figure 3). Since they describe a strong dependence of the kinetics on laser power, mainly due to singlet−triplet annihilation, the time constants reported by Savikhin and Struve[29] should be regarded as the lower limits of the actual lifetimes. Singlet−singlet annihilation processes are described by Gulbinas et al.[30] They observe that the laser power affects the amplitude of a lifetime component of 7 ps. Given a triplet lifetime of 55 μs,[16] in our measurements accumulation of triplet states was avoided by reducing the repetition frequency of the laser to 50 kHz, while the energy of the excitation pulse was as low as 0.2 nJ (10 μW, 0.03 mJ/cm^2). Hence. the laser power used in our experiments is at least 5 times lower than the lowest value used by Gulbinas et al.[30] Reducing the repetition frequency to 5 kHz also did not

change the kinetics. Therefore, we conclude that our experiments are annihilation-free.

At low temperatures the energy transfer processes appear to be slowed compared to room temperature. Although at room temperature the spectrum is equilibrated within a picosecond,[17,18] at 10 K this takes at least 37 ps. Furthermore, at low temperatures the various energy transfer steps are more distinct because of the enhanced spectral resolution and because they are also slowed. Compared to 77 K picosecond absorption difference measurements of Zhou et al.[28] on FMO of *Chlorobium tepidum*, our measurements seem to indicate that the time scale of energy relaxation is not changed drastically when going from 77 K to temperatures of 10 K or less. Recently, Gulbinas et al.[30] have concluded that spectral equilibration at 77 K takes place in 26 ps.

The four time constants, in increasing order, correspond to the lifetimes of states associated with bleachings on average at 804, 812, 815, and 823 nm in the DAS. These wavelengths are shifted by a few nanometers relative to the main features in the absorption spectrum, but this is typical for transient absorption spectra because of the contribution of stimulated emission. We conclude therefore that the bands observed in the DAS correspond to the main bands in the absorption spectrum except that the 823 nm band in the DAS is part of the red wing of the 815 nm absorption band. The actual maxima of the bands in the DAS depend somewhat on the wavelength of excitation, but this can be attributed to spectral overlap of different parts of the inhomogeneously broadened transitions with the bandwidth of excitation. (On the basis of accumulated photon echo measurements,[21−23] it has been established that the absorption spectrum of FMO is dominated by inhomogeneous broadening.) We cannot assign the time constants to energy transfer processes between specific bacteriochlorophyll molecules. Calculations have been performed to simulate the absorption spectrum of FMO complexes of *P. aestuarii*. At present there is no unambiguous assignment of the contribution of particular bacteriochlorophylls to specific bands in the absorption spectrum.[9−12,16]

Upon excitation at 790 nm, we observe that energy is very rapidly deposited in the states that give rise to bleaching at 804 and 812 nm. From there, the energy is transferred to longer wavelength states. From Figure 4C it appears that from 804 nm energy is transferred preferentially to the 815 nm state, while from the 812 nm state this occurs to the 823 nm state. However, we cannot speak of a strict selectivity. It seems more as if energy transfer is favored between states that are about 10 nm, or 120 cm^{-1}, apart. This may well be determined by the energy at which the density of (acoustic) phonon states has a maximum because one would expect that the transition probability between two states in the manifold is proportional to the density of phonon states at an energy equal to their separation, assuming that linear electron−phonon coupling is the driving mechanism for such a transition. Such a mechanism would also imply that transitions between nearly degenerate states have a relatively low probability.

The phonon density of states is a slowly varying function of frequency. If we further assume that the electron−phonon coupling strength is not, or only weakly, dependent on phonon frequency, we may conclude that the probability for a transition between two states in the exciton manifold is only weakly dependent on the energy separation, at least if they are not nearly degenerate. This means that the lifetime of a given state in the exciton manifold is to a significant degree determined by the number of states that are lower in energy, the lifetime becoming shorter as this number increases. The systematic decrease of the lifetime with increasing energy in the Q_y manifold of the FMO complex is in agreement with this conjecture.

The longest time constant of 37 ps is observed as a bleaching with a maximum at 823 nm, presumably owing to energy transfer to the 825 nm band in absorption. We note, however, that additional relaxation is observed within the 825 nm band by means of accumulated photon echo measurements, which has provided evidence that this band consists of multiple transitions.[21−23] The corresponding absorbance changes become difficult to measure because of the significant overlap of the bands involved.

The induced absorption that is associated with two-exciton transitions is clearly apparent in the decay-associated spectra in Figure 4. The amplitude of the absorbance increase to the red of the wavelength of excitation is typically on the order of 10−20% of that of the initial bleaching. The effect is most pronounced for excitation at 815 nm. These results are in qualitative agreement with excitation wavelength-dependent calculations of the excited state absorption by Van Amerongen and Struve,[31] who obtained for this contribution a value of 15−25% of the initial bleaching directly after excitation. Actually, this value is not much different from that of monomeric bacteriochlorophyll,[32] but this is to be expected if the oscillator strength is more or less evenly distributed over the exciton states in a strongly coupled system. The decay of the initially excited state to lower exciton states should also be accompanied by a rise time in the induced absorption corresponding to the lower state. This signal will show up as a bleaching, depending on the relative energies of the transitions involved. An indication of this contribution is found in the 5.5 and 37 ps spectra in Figure 4C, which show a decreased absorption that extends relatively far to the red. In other cases, this contribution may add to the bleaching of the initially excited state.

The time dependence of the anisotropy at 806 and 815 nm (Figure 5) is characterized by a very fast component with an apparent time constant of 70−100 fs and a slower component. At present, we believe that the fast component is due to a coherent artifact. The time constants of the slower component of 700 and 900 fs are somewhat different from the values measured in the isotropic decays, although the order of magnitude is very similar. A possible explanation for the difference would be the multilevel character of the first excited state of the FMO complex. It is well-known that optical excitation of a multilevel system may lead to a highly nonexponential decay, possibly with quantum-beats superposed, which strongly depends on the bandwidth of excitation.[33] These effects are caused by the loss of coherence between the different sublevels within the excitation bandwidth. The extent to which this contributes to the observations of excited state decay in FMO remains to be solved. More extensive measurements are necessary to draw definitive conclusions from the time-resolved anisotropy measurements.

Nevertheless, the anisotropy decays are markedly different from those observed by Savikhin and Struve.[29] These authors have observed strong oscillatory features in one-color pump−probe measurements with parallel and perpendicular polarizations of pump and probe beams. We note, however, that the conditions of their experiments are quite different from ours. In their experiments, because of the high repetition frequency[29] (76 MHz), combined with the triplet lifetime of 55 μs[16] and the high yield of intersystem crossing, it is difficult to avoid accumulation of a significant population of triplet states. These conditions, together with the homodyne detection technique, are highly favorable for generation and detection of accumulated photon echoes,[34,35] which may have affected their results. Note

that the possibility of observing echo signals with differently polarized beams was demonstrated by Joo et al.[36] and Hasegawa et al.[37.] We also know from experience [38] that under such conditions light scattering from the sample or from the cell windows gives rise to large oscillatory artifacts at the point of temporal overlap of the beams in the sample. This is inherent to the method of homodyne detection,[34] employed by Savikhin and Struve,[29] and may also have contributed to the oscillatory features observed by these authors. These suggestions, however, remain to be investigated in more detail.

Conclusions

With femtosecond pump−probe measurements the energy transfer in the FMO complex of *P. aestuarii* at 10 K is investigated. One- and two-color kinetics and decay-associated spectra have been obtained for different excitation wavelengths. This resulted in time constants of 0.5, 1.7, 5.5, and 37 ps corresponding to the lifetimes of the states at 804, 812, 815, and 823 nm in the decay-associated spectra, respectively. At 10 K full spectral equilibration takes about 37 ps. Anisotropy decay functions measured at different wavelengths show a ∼1 ps time constant, which might be explained by the multilevel character of the first excited state.

Acknowledgment. The authors thank C. Francke for preparation of the samples. R. J. W. Louwe wrote the global analysis program using MATLAB, which was indispensable. This work was supported by the Life Sciences Foundation (SLW), financed by The Netherlands Organization for Scientific Research (NWO).

References and Notes

(1) Fenna, R. E.; Matthews, B. W. *Nature* **1975**, *258*, 573.
(2) Kühlbrandt, W.; Wang, D. N.; Fujiyoshi, Y. *Nature* **1994**, *367*, 614.
(3) McDermott, C.; Prince, S. M.; Freer, A. A.; Hawthornthwaiteless, A. M.; Papiz, M. Z.; Cogdell, R. J.; Isaacs, N. W. *Nature* **1995**, *374*, 517.
(4) Karrasch, S.; Bullough, P. A.; Ghosh, R. *EMBO J.* **1995**, *14*, 631.
(5) Fenna, R. E.; Matthews, B. W.; Olson, J. M.; Shaw, E. K. *J. Mol. Biol.* **1974**, *84*, 231.
(6) Matthews, B. W.; Fenna, R. E.; Bolognessi, M. C.; Schmid, M. F.; Olson, J. M. *J. Mol. Biol.* **1979**, *131*, 259.
(7) Matthew, B. W.; Fenna, R. E. *Acc. Chem. Res* **1980**, *13*, 309.
(8) Tronrud, D. E.; Schmid, M. F.; Matthews, B. W. *J. Mol. Biol.* **1986**, *188*, 443.
(9) Pearlstein, R. M.; Hemenger, R. P. *Proc. Natl. Acad. Sci. U.S.A.* **1978**, *75*, 4920.
(10) Pearlstein, R. M. *Photosynth. Res.* **1992**, *31*, 213.
(11) Lu, X.; Pearlstein, R. M. *Photochem. Photobiol.* **1993**, *57*, 86.
(12) Gülen, D. *J. Phys. Chem.* **1996**, *100*, 17683.
(13) Vrieze, J. Private communication.
(14) Philipson, K. D.; Sauer, K. *Biochemistry* **1972**, *11*, 1880.
(15) Olson, J. M.; Ke., B.; Thompson, K. H. 1976 *Biochim. Biophys. Acta* **1976**, *430*, 524.
(16) Van Mourik, F.; Verwijst, R. R.; Mulder, J. M.; Van Grondelle, R. *J. Phys. Chem.* **1994**, *98*, 10307.
(17) Savikhin, S.; Zhou, W.; Blankenship, R. E.; Struve, W. S. *Biophys. J.* **1994**, *66*, 110.
(18) Savikhin, S.; Struve, W. S. *Biochemistry* **1994**, *33*, 11200.
(19) Johnson, S. G.; Small, G. J. *Chem. Phys. Lett.* **1989,** *155*, 371.
(20) Johnson, S. G.; Small, G. J. *J. Phys. Chem.* **1991**, *95*, 471.
(21) Louwe, R. J. W.; Aartsma, T. J. *J. Lumin.* **1994**, *58*, 154.
(22) Louwe, R. J. W.; Aartsma, T. J. In *Photosynthesis: From Light to Biosphere;* Mathis, P., Ed.; Kluwer Academic Publishers: Dordrecht, 1995; p 363.
(23) Louwe, R. J. W.; Aartsma, T. J. *J. Phys. Chem*., in press.
(24) Francke, C. Doctoral Thesis, University of Leiden, Leiden, The Netherlands, 1996.
(25) Asaki, M. T.; Huang, C.-P.; Zhou, J.; Kapteyn, H. C.; Murnane, M. M. *Opt. Lett.* **1993**, *18*, 977.
(26) Pshenichnikov, M. S.; De Boeij, W. P.; Wiersma, D. A. *Opt. Lett.* **1994**, *19*, 572.
(27) Beechem, J. M. In *Methods in Enzymology*; Brand, L., Hohnson, M. L., Eds.; Academic Press: San Diego 1992; Vol. 210, p 37.
(28) Zhou, W.; LoBrutto, R.; Lin, S.; Blankenship, R. E. *Photosynth. Res.* **1994**, *41*, 89.
(29) Savikhin, S.; Struve, W. S. *Photosynth. Res.* **1996**, *48*, 271.
(30) Gulbinas, V.; Valkunas, L.; Kuciauskas, D.; Katilius, E.; Liuolia, V.; Zhou, W.; Blankenship, R. E. *J. Phys. Chem.* **1996**, *100*, 17950.
(31) Van Amerongen, H.; Struve, W. S. *J. Phys. Chem.* **1991**, *95*, 9020.
(32) Becker, M.; Nagarajan, V.; Parson, W. W. *J. Am. Chem. Soc.* **1991**, *113*, 6840.
(33) Kommandeur, J. In *Advances in Chemical Physics*; Prigogine, I., Rice, S. A., Eds.; Wiley: New York, 1988; Vol. 70, p 133.
(34) Aartsma, T. J.; Louwe, R. J. W.; Schellenberg, P. In *Biophysical Techniques in Photosynthesis*; Amesz, J., Hoff, A. J., Eds.; Kluwer Academic Publishers: Dordrecht, 1996; Chapter 7.
(35) Hesselink, W. Doctoral Thesis, University of Groningen, Groningen, The Netherlands, 1980.
(36) Joo, T.; Jia, Y.; Yu, J.; Jonas, D. M.; Fleming, G. R. *J. Phys. Chem.* **1996** *100*, 2399.
(37) Hasegawa, A.; Mitsumori, Y.; Minami, F. *J. Lumin*. **1996**, *66*−*67*, 51.
(38) Louwe, R. J. W. Private communication.